Supporting Information

Raising the solubility of Gd yields superior thermoelectric performance in *n*-type PbSe

Qian Deng,[a] Yan Zhong,[a] Canyang Zhao,[a] Fujie Zhang,[a] Cheng-Liang Xia,[b] Yue Chen,[b] and Ran Ang*[ac]

[a]Key Laboratory of Radiation Physics and Technology, Ministry of Education, Institute of Nuclear Science and Technology, Sichuan University, Chengdu 610064, China

[b]Department of Mechanical Engineering, The University of Hong Kong, Pokfulam Road, Hong Kong SAR, China

[c]Institute of New Energy and Low-Carbon Technology, Sichuan University, Chengdu 610065, China

*Corresponding author and Email: rang@scu.edu.cn

Computational details

Electrical transport modeling

The density of state mass m^* and Lorenz number L were calculated based on single parabolic band (SPB) model by the following equations:

$$S = \frac{k_b}{e}\left[\frac{(r+5/2)F_{r+3/2}(\eta)}{(r+3/2)F_{r+1/2}(\eta)} - \eta\right] \quad \text{(eq. S1)}$$

$$n_H = \frac{4\pi}{A}\left[\frac{2m^* k_B T}{h^2}\right]^{3/2} F_{1/2}(\xi) \quad \text{(eq. S2)}$$

$$A = \frac{3}{2}F_{1/2}(\eta)\frac{F_{-1/2}}{2F_0^2} \quad \text{(eq. S3)}$$

$$L = \frac{\kappa_B^2 3F_0F_2 - 4F_1^2}{e^2 \quad F_0^2} \quad \text{(eq. S4)}$$

$$F_n(\xi) = \int_0^\infty \frac{x^n}{1+e^{(x-\xi)}}dx \quad \text{(eq. S5)}$$

Here, k_B is the Boltzmann constant, F_n is the Fermi integral, and the reduced chemical potential is given by $\xi = E_F/(k_B T)$, where E_F is the Fermi energy.

Thermal transport modeling

The lattice thermal conductivity (κ_{lat}) of alloys was calculated by the modified Debye-Callaway model[1], which can be expressed by the equation (6).

$$\kappa_{lat} = \frac{K_B}{2\pi^2 \upsilon}\left(\frac{K_B}{\hbar}\right)^3 \int_0^{\Theta/T} \tau_{tot}(x)\frac{x^4 e^x}{(e^x-1)^2}dx \quad \text{(eq. S6)}$$

Here, υ is the average speed of phonon, $\hbar$ is the reduced Planck constant, Θ is the Debye temperature, x is the relation of $\hbar\omega/k_B T$, ω is the phonon frequency, and τ_{tot} is the total phonon scattering relaxation time. τ_{tot} can be attributed to scattering from various mechanisms such as normal (N) and Umklapp (U) processes, point defects (PD), nanoprecipitates (NP), boundaries (B), dislocation cores (DC), and dislocation strains (DS) according to the Matthiessen's equation $\tau_{tot}^{-1} = \tau_U^{-1} + \tau_N^{-1} + \tau_{PD}^{-1} + \tau_{NP}^{-1} + \tau_B^{-1} + \tau_{DS}^{-1} + \tau_{DC}^{-1}$.The phonon scattering relaxation time for respective mechanism can be expressed as follows:

Umklapp phonon scattering

$$\tau_U^{-1} = A_N * \frac{2 \quad K_B \bar{V}^{1/3} \omega^2 \gamma^2 T}{(6\pi^2)^{\frac{1}{3}} \quad \bar{M}\upsilon^3} \quad \text{(eq. S7)}$$

Normal phonon scattering

$$\tau_N^{-1} = \frac{2 \quad K_B \bar{V}^{1/3} \omega^2 \gamma^2 T}{(6\pi^2)^{\frac{1}{3}} \quad \bar{M} v^3} \qquad \text{(eq.S8)}$$

Point defect phonon scattering

$$\tau_{PD}^{-1} = \frac{\bar{V}\omega^4}{4\pi^3 v^3} * \sum (1-x_i)\left[\left(\frac{M_i - M}{M}\right)^2 + \varepsilon\left(\frac{a_i - a}{a}\right)^2\right] \qquad \text{(eq. S9)}$$

Precipitates scattering

$$\tau_{NP}^{-1} = v(\sigma_s{}^{-1} + \sigma_L{}^{-1})^{-1} V_p \qquad \text{(eq. S10)}$$

Boundaries scattering[2]

$$\tau_B^{-1} = \frac{v}{d} \qquad \text{(eq. S11)}$$

Dislocation scattering that includes both dislocation core (τ_{DC}) and dislocation strain(τ_{DS}) scattering.

$$\tau_{DC}^{-1} = N_D \frac{\bar{V}^{4/3}}{v^2} \omega^3 \qquad \text{(eq. S12)}$$

$$\tau_{DS}^{-1} = A' N_D \gamma^2 B_D{}^2 \omega \left\{\frac{1}{2} + \frac{1}{24}\left(\frac{1-2\nu}{1-\nu}\right)^2 \left[1 + \sqrt{2}\left(\frac{v_L}{v_T}\right)^2\right]^2\right\} \qquad \text{(eq. S13)}$$

In above equations, $\bar{V}$ is the average atomic volume, $\bar{M}$ is the average atomic mass, γ is the Grüneisen parameter, A_N is the ratio between normal process and Umklapp phonon scattering, N_D is the number of dislocations (or stacking faults) crossing a line of unit length, B_D is the magnitude of the Burgers vector of the dislocation.

Estimation of dislocation density

To quantitatively understand the structural characteristics within our Gd and Br co-doped PbSe sample, we further estimate the dislocation density using $N_D = L/Ad$, where the L and A are respectively the total length of recognized dislocation line and the area of the captured TEM image and d is the specimen thickness.

As the TEM specimen was prepared by FIB, the average thickness of the prepared cross-sectional specimen d was estimated as 100 nm and the observation area can be determined as 25 μm^2 (5 μm in length and 5 μm in width) based on our precise sample preparation process, considering the geometry of obtained lamella. To statistically estimate the dislocation density in our samples, different areas in the sample were carefully examined in the HRTEM imaging. Consequently, the dislocation density in our $Pb_{0.997}Gd_{0.003}Br_{0.003}Se_{0.997}$ sample can be estimated as ~4×10^{11} cm^{-2}.

Supplementary details

Figure S1. The back-scattered electron images of $Pb_{0.994}Gd_{0.006}Se$ sample and the corresponding EDS mapping, showing obvious precipitates.

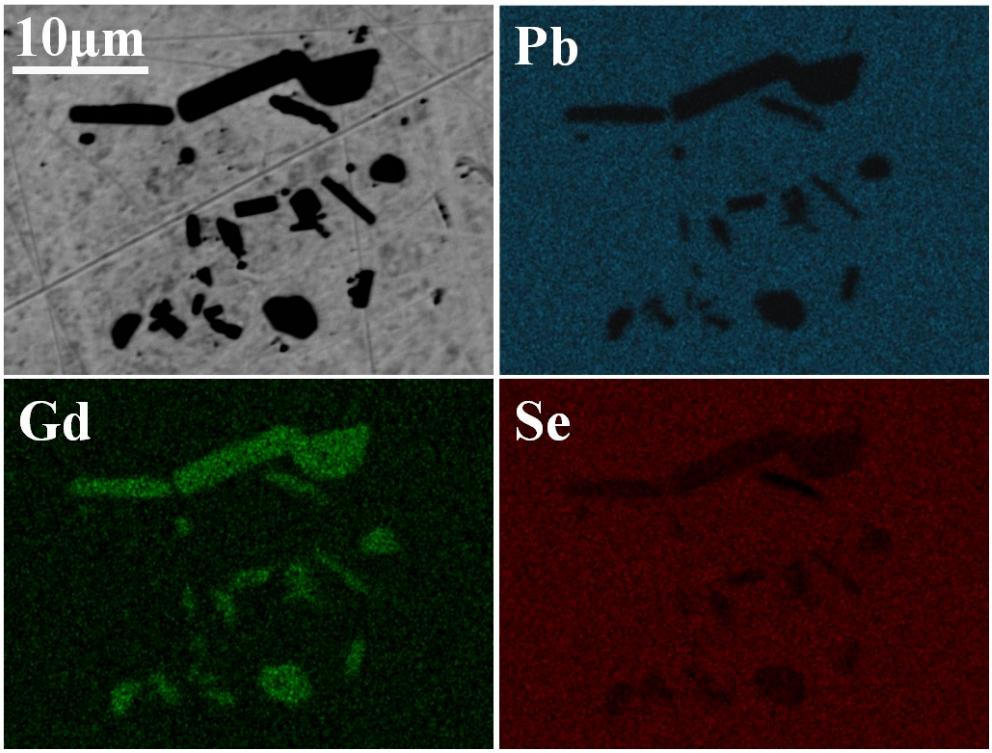

Figure S2. EDS point scanning of $Pb_{0.994}Gd_{0.006}Se$ sample from Fig. S1, confirming that the precipitates are the selenium-gadolinium compounds.

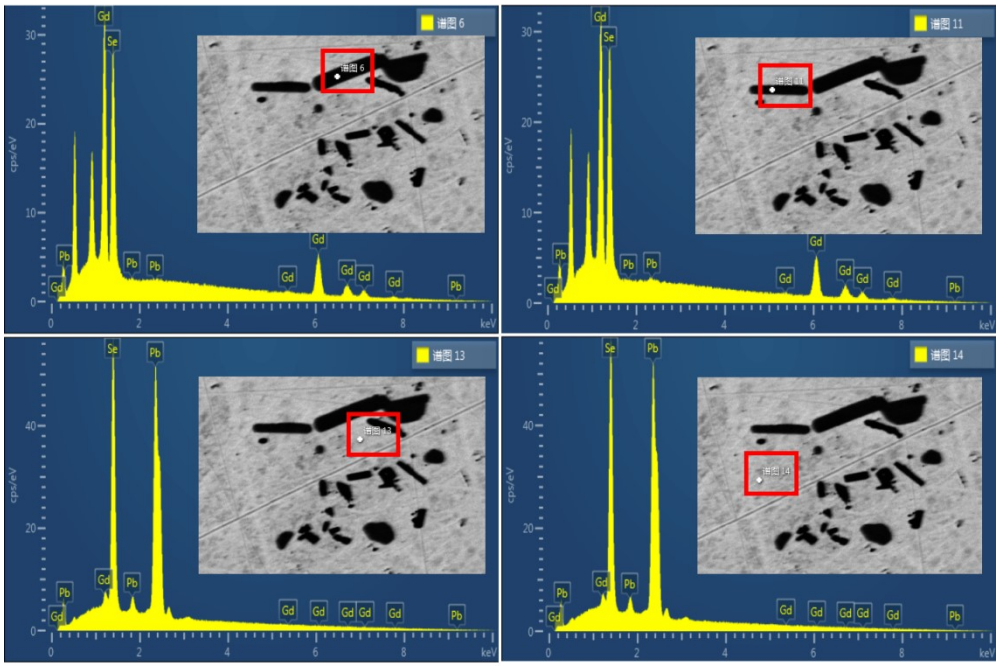

Figure S3. The measured Hall carrier density as a function of Gd concentration. The black and red circles are the measured values. The blue circles represent the calculated predictions based on simple valence principle.

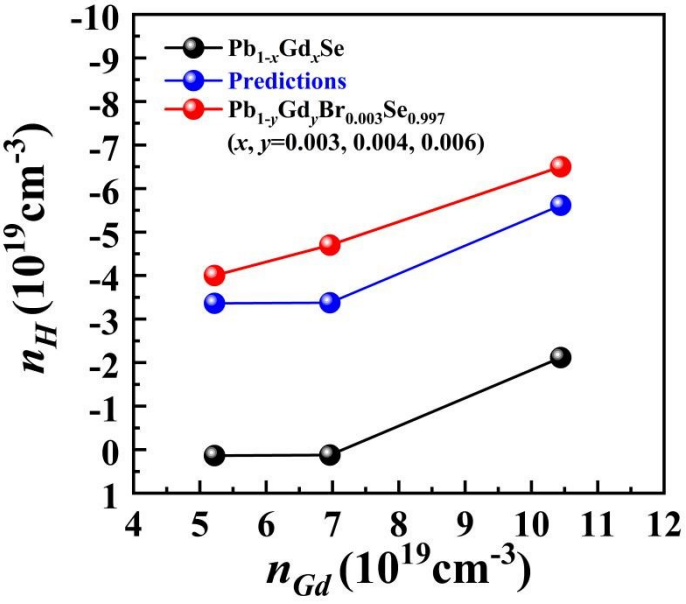

Figure S4. Typical medium-magnification TEM image of the $Pb_{0.997}Gd_{0.003}Br_{0.003}Se_{0.997}$ sample indicates the dislocations.

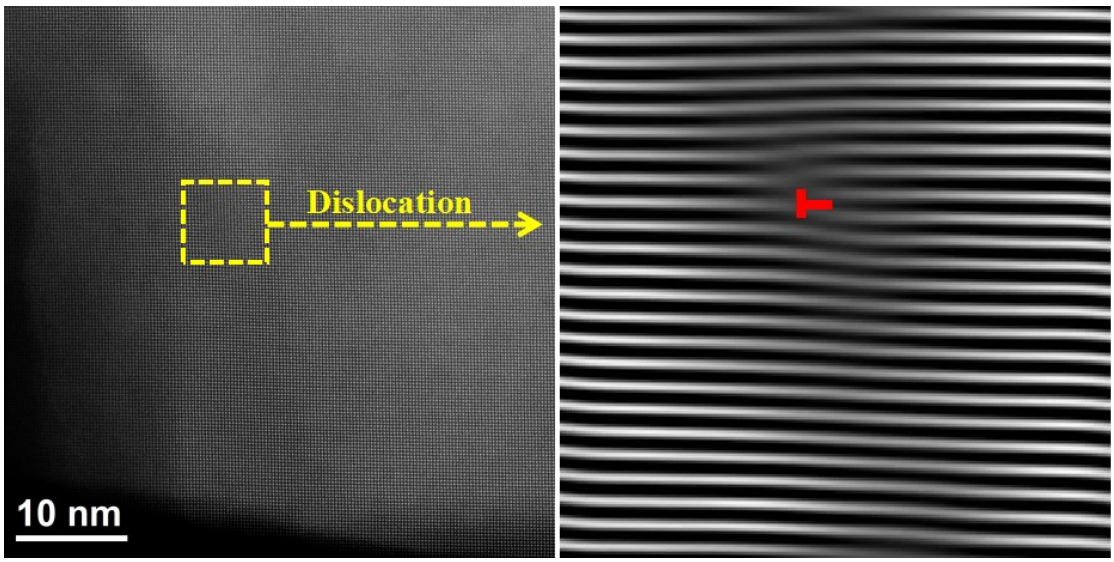

Figure S5. GPA strain distributions for specific region of $Pb_{0.997}Gd_{0.003}Br_{0.003}Se_{0.997}$ sample. It corresponds to Figure 6g.

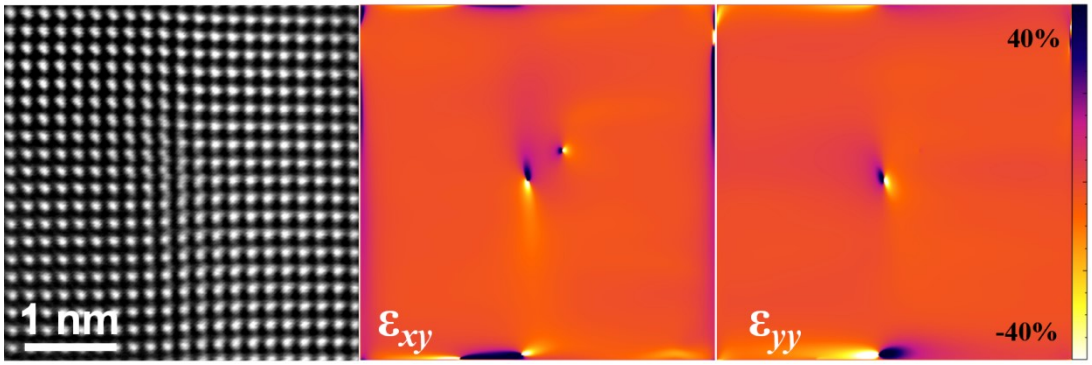

Figure S6. The temperature dependence of thermal diffusivity for $Pb_{1-y}Gd_yBr_{0.003}Se_{0.997}$ (y=0.002-0.006) samples.

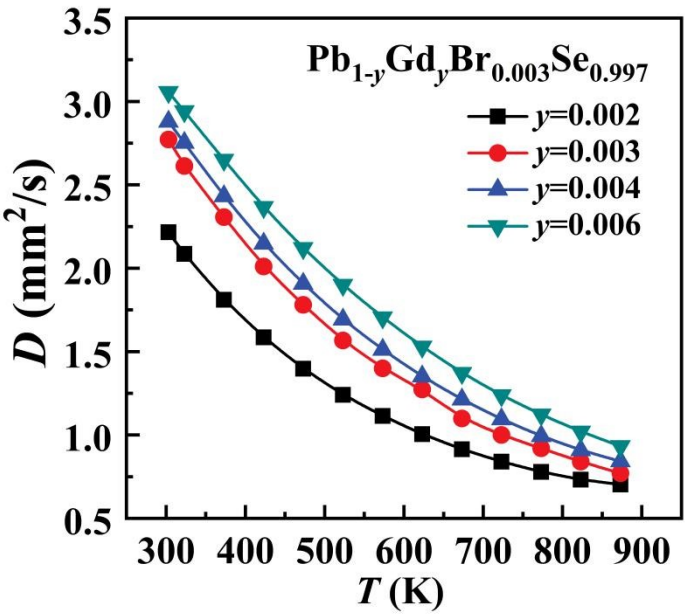

Supplementary Tables

Table S1. The experimentally measured transport properties of $Pb_{1-x}Gd_xSe$. The samples change from *p*-type to *n*-type with increasing Gd content.

Samples	303 K				873 K				
	n_H ($10^{18}cm^{-3}$)	μ_H ($cm^{-2}V^{-1}S^{-1}$)	PF ($mWm^{-1}K^{-2}$)	κ_{tot} ($WK^{-1}m^{-1}$)	n_H ($10^{18}cm^{-3}$)	μ_H ($cm^{-2}V^{-1}S^{-1}$)	PF ($mWm^{-1}K^{-2}$)	κ_{tot} ($WK^{-1}m^{-1}$)	zT_{max}
***x*=0.002**	1.75	82	0.12	1.72	-5.9	-57	2.4	1.31	0.15
***x*=0.003**	1.40	269	1.7	1.71	-9.9	-38	3.4	1.29	0.19
***x*=0.004**	1.30	54	0.15	1.67	-11	-44	4.3	1.22	0.30
***x*=0.006**	-19	-21	0.2	2.27	-19	-47	7.1	1.08	0.54

Table S2. The sample densities of $Pb_{1-x}Gd_xSe$ and $Pb_{1-y}Gd_yBr_{0.003}Se_{0.997}$ measured by Archimedes method. The theoretical density of pure PbSe is 8.1 g cm^{-3}.

systems	Samples	Measured density(g cm^{-3})	Relative density (%)
$Pb_{1-x}Gd_xSe$	***x*=0.002**	8.09	99.75
	***x*=0.003**	8.07	99.62
	***x*=0.004**	7.93	97.90
	***x*=0.006**	7.84	96.79
$Pb_{1-y}Gd_yBr_{0.003}Se_{0.997}$	***y*=0**	8.06	99.51
	***y*=0.002**	8.04	99.26
	***y*=0.003**	8.00	99.14
	***y*=0.004**	7.96	98.27
	***y*=0.006**	7.94	98.02

Table S3. Parameters used to calculate κ_{lat} based on various phonon scattering processes.

Paramaters	symbol	Values	Ref
Atomic mass of matrix (g mol^{-1})	M_i	207.2 (Pb) 78.96 (Se)	
Atomic mass of impurities (g mol^{-1})	M	157.25 (Gd) 79.9 (Br)	
Lattice parameters for $Pb_{1-y}Gd_yBr_{0.003}Se_{0.997}$ (Å)	a_i	6.125-0.1667*y	This work
Average atomic mass (kg)	$\bar{M}$	M/(2×6.023×10^{23})	This work
Average atomic mass volume (Å^3)	$\bar{V}$	$a_i^3/8$	
Boltzmann constant (J/K)	K_B	1.38×10^{-23}	
Grüneisen parameter	γ	1.7	[3]
Average sound velocity (m/s)	v	1787	[4]
Longitudinal velocity (m/s)	v_L	3150	[4]
Transverse velocity (m/s)	v_T	1600	[4]
Debye temperature (K)	Θ	193	[5]
Umklapp to normal ratio	A_N	4	[6]
Pre-factor for dislocation scattering	A'	0.96	[7]
Poisson ratio	r	0.243	
Phenomenological parameter	ε	64	[8]
Burgers vector (m)	B_D	4.33×10^{-10}	[4]
Dislocation density for $Pb_{1-y}Gd_yBr_{0.003}Se_{0.997}$ (cm^{-2})	N_D	4×10^{11} (y=0.003)	This work

1. J. Callaway and H. C. Vonbaeyer, *Phys. Rev.*, 1960, **120**, 1149-1154.
2. D. T. Morelli, J. P. Heremans and G. A. Slack, *Phy. Rev. B*, 2002, **66**, 195304.
3. T. Grandke, M. Cardona and L. Ley, *Solid State Commun.*, 1979, **32**, 353-356.
4. Z. Chen, B. Ge, W. Li, S. Lin, J. Shen, Y. Chang, R. Hanus, G. J. Snyder and Y. Pei, *Nat. Commun.*, 2017, **8**, 13828.
5. C. Zhou, Y. K. Lee, J. Cha, B. Yoo, S. P. Cho, T. Hyeon and I. Chung, *J. Am. Chem. Soc.*, 2018, **140**, 9282-9290.
6. H. Wang, Y. Pei, A. D. LaLonde and G. J. Snyder, *Proc. Natl. Acad. Sci. U. S. A.*, 2012, **109**, 9705-9709.
7. W. R. G. Kemp, P. G. Klemens and R. J. Tainsh, *Philos. Mag.*, 1959, **4**, 845-857.
8. H. Wang, J. Wang, X. Cao and G. J. Snyder, *J. Mater. Chem. A*, 2014, **2**, 3169-3174.